JOURNAL OF PHYSIOLOGY AND PHARMACOLOGY 2021, 72, 6, 857-871
www.jpp.krakow.pl | DOI: 10.26402/jpp.2021.6.04

W. KOZLOWSKA[1], E.M. DRZEWIECKA[1], L. PAUKSZTO[2], A. ZMIJEWSKA[1], P.J. WYDORSKI[1], J.P. JASTRZEBSKI[3], A. FRANCZAK[1]

EXPOSURE TO THE ELECTROMAGNETIC FIELD ALTERS THE TRANSCRIPTOMIC PROFILE IN THE PORCINE ENDOMETRIUM DURING THE PERI-IMPLANTATION PERIOD

[1]Department of Animal Anatomy and Physiology, Faculty of Biology and Biotechnology, University of Warmia and Mazury in Olsztyn, Olsztyn, Poland; [2]Department of Botany and Nature Protection, Faculty of Biology and Biotechnology, University of Warmia and Mazury in Olsztyn, Olsztyn, Poland; [3]Department of Plant Physiology, Genetics and Biotechnology, Faculty of Biology and Biotechnology, University of Warmia and Mazury in Olsztyn, Olsztyn, Poland

A low-frequency electromagnetic field (EMF) is an environmental pollutant that may influence female reproduction. This research was undertaken to test the hypothesis that EMF causes alterations in the transcriptomic profile of the endometrium. This study investigated the *in vitro* effects of EMF treatment (50 Hz, 2 h) on global transcriptome alterations in the endometrium isolated from pigs during the peri-implantation period. The control endometrium was not treated with EMF. The EMF treatment altered the expression of 1561 transcriptionally active regions (TARs) in the endometrium. In the group of 461 evaluated DEGs, 156 were up-regulated (34%), 305 were down-regulated (66%) and 341 (74%) had known biological functions. A total of 210 long noncoding RNAs (lncRNAs) with changes in expression profiles, and 146 predicted RNA editing sites were also evaluated. Exposure to EMF changes the expression of genes encoding proteins that are involved in proliferation and metabolism in endometrial tissue. These results provide useful inputs for further research into the impact of EMF on molecular changes in the uterus during the peri-implantation period and, consequently, pregnancy outcome.

Key words: *electromagnetic field, porcine endometrium, pregnancy, transcriptome, differentially expressed genes, long non-coding RNA, gene ontology annotations, apelin signaling*

INTRODUCTION

Living organisms are exposed daily to an electromagnetic field (EMF), commonly at a frequency of 50 Hz, which is generated by wires or household devices (1, 2). The exposure to EMF affects and alters many physiological processes in animals, including cell differentiation and proliferation, immune responses, brain activity, memory processes and reproductive functions (1, 3-15).

An EMF is recognized as an environmental pollutant that induces alterations in the activity of uterine tissues in pregnant and cyclic females (5, 6, 14, 15). The intensity, strength, and duration of EMF can cause various hazardous effects (16, 17). It was documented that *in vitro* exposure to 50 Hz EMF treatment lasting 2 to 4 h affects the synthesis and secretion of steroid hormones in the uterus (5, 6, 14, 15). Research also provided new insights into the mechanisms of EMF action in the regulation of the transcriptomic profile of the porcine myometrium during the peri-implantation period (4). It would be interesting to determine whether EMF treatment alters the transcriptomic profile of the endometrium and induces changes that may disturb the proper course of molecular mechanisms in the uterus during the peri-implantation period.

The peri-implantation period is a crucial stage for successful pregnancy establishment in many species. At the beginning of the implantation, one-third of embryos can be lost (18-20). Therefore, the exposure of uterine tissue to EMF during the fetal peri-implantation period may have highly undesirable consequences. The study tested the hypothesis that EMF treatment during the peri-implantation period alters the transcriptomic profile of the endometrium.

The proper activity of the endometrium is important for the creation of embryo-maternal molecular dialog during the peri-implantation period. The endometrium offers an immune-privileged and nutritive milieu that are essential for embryo and placental development (21-25). In the present study, EMF-induced changes in the endometrium were extensively analyzed by examining the impact of a 2-hour EMF treatment at a frequency of 50 Hz on the transcriptomic profile of porcine tissues collected during the peri-implantation period, *i.e.* on days 15 to 16 of pregnancy. The short exposure (2 hours) to EMF at a frequency of 50 Hz occurs commonly in the environment (1, 2). The study focused on: 1) up- and down-regulated genes with known biological functions, 2) differentially expressed non-coding RNAs (DE-ncRNAs), 3) network of interactions between selected groups of genes, 4) gene ontology (GO), 5) biological pathways (Kyoto Encyclopedia of Genes and Genomes, KEGG), and 6) single nucleotide variants (SNV) identified in the endometrium as a result of EMF treatment. The molecular

background of transcriptomic changes induced by short-term EMF treatment of the endometrium during the peri-implantation period was taken into consideration in the analysis.

MATERIALS AND METHODS

Ethical statement

All experiments were conducted on animal tissues collected post-mortem during regular slaughter procedures in a professional slaughterhouse (Rozdroze, Poland). Living pigs were not handled by the authors. According to the legislation of the European Union (Directive 2010/63/EU of the European Parliament and the Council, Article 3 [Definitions], paragraph 1) and Polish law (Act of 15 January 2015, Article 2, paragraph 1, point 6), the approval of an ethics committee is not required for research conducted on animal tissues.

Animals, collection of endometrial tissues and electromagnetic field exposure system

Post-pubertal pigs (*Sus scrofa domestica* L.), Polish Landrace × Polish Large White weighing 95 to 110 kg, were naturally mated on the first and the second day of estrus. Second mating was recognized as the first day of pregnancy. All experimental procedures were performed on fragments of the endometrium that had been prepared according to the method previously described by Kozlowska *et al.* (6). Briefly, endometrial tissue was collected from pigs (n = 6) during the peri-implantation period, *i.e.* on days 15 to 16 of pregnancy. Endometrial slices were standardized (thickness: 2 to 3 mm; weight: 95 to 105 mg each) and incubated *in vitro*. Specifically, endometrial fragments were first preincubated in a 24-well culture plate containing 1 mL of the M199 culture medium (Sigma Aldrich, Gillingham, Dorset, U.K., M2520-10x1L), 0.1% bovine serum albumin (Carl Roth GmBH + Co KG, Karlsruhe, Germany, 8076.3), 1% antibiotic - antimycotic solution (Sigma Aldrich, St. Louis, MO, USA, A5955-100ML) in a water-shaking bath at 37ºC (95% O_2 and 5% CO_2) for 2 h. Subsequently, the preincubation medium was replaced with fresh medium, and endometrial slices were incubated for 2 h in the presence and absence of EMF at a frequency of 50 Hz. The EMF was generated by the Astar generator (Magneris, Astar https://www.astar.pl/produkty/ magneris) equipped with applicators. An EMF exposition system was designed with the technical requirement of the generator. The EMF exposure system and the reasons for applying the EMF treatment at a frequency of 50 Hz for 2 h, and magnetic induction of 8 mT had been explained previously in detail by Koziorowska *et al.* (14). After incubation, endometrial slices were collected, snap-frozen in liquid nitrogen (–196ºC), and stored at –80ºC for further transcriptomic analyses.

RNA isolation

Total RNA was extracted from the endometrium following combined protocols involving the TRI Reagent (Sigma Aldrich, St. Louis, MO, USA, T9424-100ML) and the RNeasy Mini Kit (Qiagen, Germantown, MD, USA, 74106), as described by Drzewiecka *et al.* (4). In brief, the endometrium (20 µg) was precisely shredded on ice in DEPC-treated (MP Biomedicals, Eschwege, Germany, 0215090280) Eppendorf tubes containing the TRI Reagent (500 µl). Homogenization of the tissue was performed with the TissueRuptor homogenizer (Qiagen, Germantown, MD, USA) for 2 s, and the samples were vortexed for 10 s. Subsequently, the samples were incubated on ice for 30 min and quickly vortexed after every 10 min of incubation until digestion was achieved. Thereafter, ice-cold chloroform (150 µl) was added to each sample and mixed by pipetting. Samples were incubated for 3 minutes and then centrifuged at 8000 × g for 8 min at 4ºC. The upper phase was transferred to another Eppendorf tube with 200 µl of 70% ethanol cooled to –20ºC and mixed using pipete. Samples were transferred thoroughly onto the RNeasy Mini spin column (Qiagen, Germantown, MD, USA, 74106), incubated (1 min) and centrifuged for 15 s at 8000 × g at room temperature (RT). After RNA binding to column membranes, RNA was isolated according to the manufacturer's protocol (Qiagen, Germantown, MD, USA). RNA was eluted using 80 µl of DEPC-treated water. The initial purity (optical density, OD: A260/A280) and concentration of the obtained RNA were measured spectrophotometrically. Samples with an OD of 1.8 to 2.0 and a concentration of > 500 ng/µL were used in further analyses. Aliquots of the obtained RNA were frozen at –80ºC. RNA integrity number (RIN: 28 S/18 S ratio) was measured using the Agilent 2100 Bioanalyzer with the RNA 6000 Nano LabChip kit (Agilent Technologies, Santa Clara, CA, USA), for next-generation sequencing (NGS) (Macrogen, Seoul, South Korea), and for future validation of the results of NGS analyses. Only samples with RIN ≥ 7.5 were selected for further analyses. Each aliquot was used only once throughout the freezing-refreezing cycle. Finally, three control (not treated with EMF) and three experimental (EMF-treated) samples with the highest RINs were selected for the NGS procedure.

Construction and sequencing of cDNA libraries - next-generation sequencing

The construction and sequencing of cDNA libraries were performed by Macrogen (Seoul, South Korea) in the Illumina NovaSeq 6000 System (Illumina, San Diego, CA, USA). Briefly, the prepared RNA aliquots (RIN ≥ 7.5 rRNA ratio ≥ 1.0 concentration > 20 ng/µL, total content > 1 µg, total volume > 50 µL) were used to construct TruSeq mRNA stranded libraries for further sequencing using the NovaSeq 6000 platform, with a read length configuration of 2 × 150 bp and a throughput of 40M reads per sample. Raw data were submitted to the European Nucleotide Archive (ENA) under accession No. PRJEB50034, and used for transcriptome profiling and gene expression analysis.

Transcriptome profiling and bioinformatic analysis of gene expression

A Principal Components Analysis (PCA), differentiation analysis and gene expression profiling were performed for control (n = 3) and experimental (n = 3) RNA-seq libraries, as previously described in detail by Paukszto *et al.* (26) and Drzewiecka *et al.* (4). In brief, digital sequences of paired-end reads were saved in FASTQ format and evaluated with FASTQC software v. 0.11.7 (27). The quality control procedure was performed in Trimmomatic software v. 0.38 (28), and low-quality reads (with a PHRED cutoff score ≤ 20 in a 10 bp frameshift sequence) were removed. The remaining clean paired-end reads were aligned to the pig reference genome with ENSEMBL annotation (Sus_scrofa.Sscrofa11.1.98), using the STAR v.2.7.3 mapper (29) and the StringTie v. 1.3.3 (30) pipeline. The count values obtained in the mapping procedure (-quantMode GeneCounts; STAR attribute) were assigned to transcriptionally active regions (TARs). Porcine TARs were separated into uncovered regulatory transcripts and protein-coding genes. Differential expression of genes was assessed with statistical methods: edgeR (31) and DESeq2 (32).

Transcripts that were identified as differentially expressed TARs (DE-TARs) had an adjusted *p*-value < 0.05 and an absolute value of logarithmic Fold Change (log2FC) > 1, determined by both methods. DE-TARs were divided into differentially expressed genes (DEGs) and differentially expressed noncoding transcripts (DE-ncRNAs). Next, the evaluated DEGs were classified into gene ontology (GO) terms and biological pathways using the Kyoto Encyclopedia of Genes and Genomes (KEGG) (33-35) in gProfiler software (36). The enrichment of functional classification was performed at the adjusted *p*-value < 0.05. The final consensus DEGs were visualized in MA, Volcano, and Circos heatmaps with gplots circlize Bioconductor v. 3.13 package, and a custom script in R v. 4.1.1. The identified DE-ncRNAs were divided into differentially expressed long noncoding RNAs (DE-lncRNAs) and other unclassified DE-ncRNAs. The pool of DE-lncRNAs included transcripts with ENSEMBL lncRNA biotype, uncovered transcripts (length > 200 bp), multi-exonic structure and no protein-coding potential. The coding potential was tested by three algorithms: the Coding-Potential Assessment Tool (CPAT) (37), a predictor of long non-coding RNAs and messenger RNAs based on an improved k-mer scheme (PLEK) (38) with default parameters, and the Coding Potential Calculator (CPC2) (39). The correlation (*trans*-acting links) between the expression of DE-lncRNAs and DEGs was examined in a custom R script. The *trans*-acting relationship was established based on the calculated values of Pearson's correlation coefficient for the expression profiles (positive correlation r > 0.9, or negative correlation r < –0.9).

RNA editing site prediction

The single nucleotide variant (SNV) calling procedure was performed with python rMATS-DVR scripts (40). The reference and alternative allele frequencies (AAF) of the identified SNVs were calculated with the Picard tool (Broad Institute, Picard; http://broadinstitute.github.io/picard, accessed 19 Sept 2018) and the golden-standard Genome Analysis Tool Kit (GATK) (41) in the rMATS-DVR pipeline. The applied pipeline supported the identification of nucleotide sites with AAF differences between EMF-treated and control samples. Using ENSEMBL VCF and GTF files, single nucleotide polymorphisms (SNPs) were annotated and gene locations were assigned to the expressed variants. The obtained SNVs were filtered out according to the GATK standard parameters: depth coverage < 10; RMSMappingQuality < 40; QualitybyDepth < 2; Mapping QualityRankSum < –12.5; and ReadPosRankSum < –8. High-quality SNVs with alternative allele occurrence in at least half RNA-seq samples were used in the downstream analysis. The SNVs situated in the vicinity of spliced junction sites within bidirectional genes and pseudogenes were removed from the analysis of the predicted RNA editing sites. The AAF alterations (ΔAAF > 0.1; FDR < 0.001) between EMF-treated and control samples were assessed only for canonical RNA editing substitutions. The allelic imbalance ratio was determined in the chi-square goodness-of-fit test in the R environment, and RNA editing candidates were annotated in Variant Effect Predictor (VEP) (42) and plotted in Circos (43).

Validation procedure

The validation procedure was done by comparing the relative mRNA transcript abundance (Real-Time PCR) of 10 selected DEGs (five up-regulated and five down-regulated) in the endometrial slices exposed *in vitro* to EMF at 50 Hz vs. the control. DEGs were selected for validation based on their FC values and contribution to the evaluated GO terms. The selected DEGs were: early growth response 2 (*EGR2*), hydroxysteroid 17β dehydrogenase 2 (*HSD17B2*), inhibitor of DNA binding 2 (*ID2*), interferon-gamma receptor 1 (*IFNGR1*), interleukin 1 receptor accessory protein (*IL1RAP*), melanocortin 2 receptor accessory protein 2 (*MRAP2*), nitric oxide synthase 3 (*NOS3*), prostaglandin E receptor 4 (*PTGER4*), serpin family E member 1 (*SERPINE1*), and vitamin D receptor (*VDR*). In the selected DEGs, mRNA was amplified with the TaqMan™ RNA-to-CT™ 1-Step Kit and specific, pre-designed TaqMan™ probes presented in *Table 1* (both supplied by Thermofisher Scientific, Waltham, MA, USA). The amplification was performed in an AriaMX apparatus (Agilent Technologies, Wood Dale IL, USA) using 4 pg/µl of total RNA (10 µl of total reaction volume). The analysis relied on the general guidelines for gene expression analysis (44) and the manufacturer's protocol. The relative abundance of the mRNA transcript was calculated using the ΔΔCt method, and statistically significant differences were evaluated with the t-test in the Statistica program (StatSoft Inc., Tulsa, OK, USA).

Table 1. Taq Man probes used in the validation of next-generation sequencing (NGS) results in the experiment.

Fold Change[1]	Gene Symbol	Assay ID
Differentially expressed genes		
–2.924716450	*EGR2*	Ss03388929_m1
–2.460743857	*HSD17B2*	Ss04245816_m1
–1.803136846	*ID2*	Ss03379795_u1
2.685030595	*IFNGR1*	Ss04246620_m1
–2.771015013	*IL1RAP*	Ss06918537_m1
3.402965564	*MRAP2*	Ss06896222_m1
1.967100363	*NOS3*	Ss03383840_u1
–1.889229989	*PTGER4*	Hs00168761_m1
1.908155139	*SERPINE1*	Ss03392656_u1
3.628050729	*VDR*	Ss03385197_u1
Reference genes		
-	*ACTB*	Ss03376081_u1
-	*GAPDH*	Ss03374854_g1

[1]Fold change ($p \leq 0.05$) obtained after transcriptome profiling NGS analysis.

RESULTS

Statistical analysis of RNA sequencing data

The overall RNAseq dataset was built for six cDNA libraries (three for the endometrium exposed to EMF, and three for control samples). A total of 329,577,212 raw paired reads were obtained after sequencing (average of 54,929,535 per sample) (*Table 2*). 263,807,006 of 311,761,610 filtered reads were mapped to the porcine genome (Ss11.1.98), and the unique mapping rate ranged from 67% to 90%. The following proportions of reads were mapped to gene structures: 42.13% of

Table 2. The results of sequencing, trimming and mapping six RNA-seq libraries extracted from the porcine endometrium that was and was not exposed to electromagnetic field (EMF) at 50 Hz for 2 h.

	End_CTR1	**End_CTR2**	**End_CTR3**	**End_EMF1**	**End_EMF2**	**End_EMF3**
Row reads	66266972	49397438	56200292	58258060	52247674	47206776
Trimmed reads	62775170	46434842	52854782	56177314	49210070	44309432
Mapped	54095556	38396366	45815510	52564960	38321540	34613074
Uniquely mapped	52544786	36096918	44120998	51017982	32919888	32640056
Multi-mapped	1455166	2256456	1651576	1518462	5367178	1942642
Too many loci	95604	42992	42936	28516	34474	30376

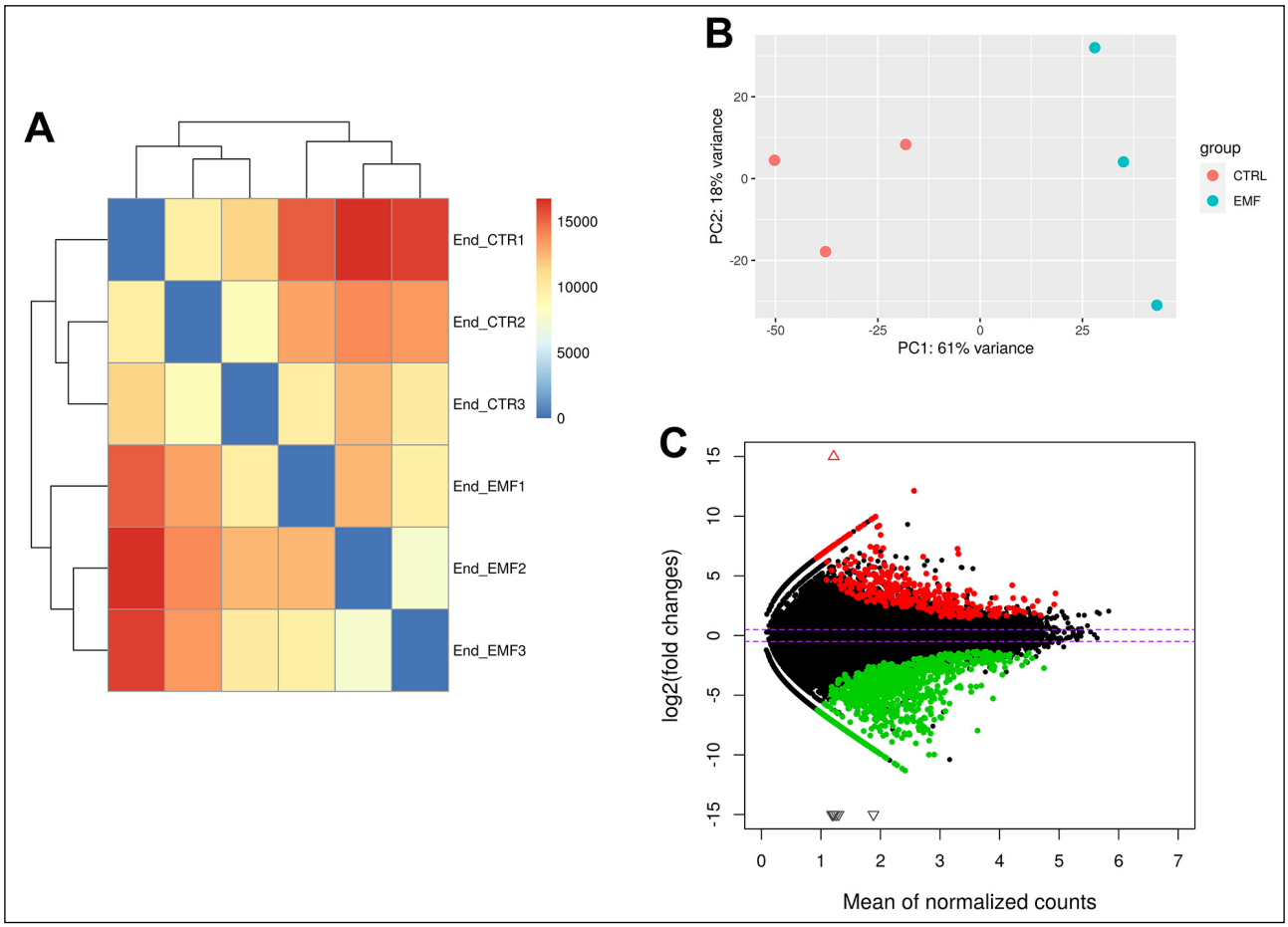

Fig. 1. Transcriptome-wide RNA-seq analysis and expression profiles of differentially expressed active regions (DE-TARs) in the endometrium after electromagnetic field (EMF) exposure. Poisson distance matrices (Pheatmap) of the transcriptomic profiles of the porcine endometrium exposed to EMF (A). Principal component analysis (PCA) of 6 libraries of RNA sequences isolated from the endometrium (three treated by EMF - blue circle; and three controls - red circles); the X-axis describes the results of principal component 1 and the Y-axis describes the results of principal component 2 (B). The MA plot presents the logarithmic scale of fold changes on the Y-axis and normalized expression count values on the X-axis (C). Red dots represent upregulated DE-TARs, green dots describe downregulated DEGs.

reading pairs were mapped to coding sequences, 26.41% were aligned to untranslated regions, 18.33% to intergenic regions, and 13.13% to introns. The transcriptomic profiles of biological replicates in EMF-treated and control groups were visualized in Pheatmap and PCA (*Fig. 1A* and *1B*, respectively).

Identification of differentially expressed genes (DEGs) and differentially expressed non-coding RNAs (DE-ncRNAs)

The expression of 1561 DE-TARs, including 1100 noncoding transcripts, was altered in the EMF-treated endometrium. DE-TARs are presented in MA plots in *Fig. 1C*. In the ENSEMBL database, 461 of the identified DE-TARs were annotated as protein-coding genes (*Fig. 2*). In the group of down-regulated and up-regulated DE-TARs, 305 and 156 transcripts were annotated as protein-coding genes, respectively. In the EMF-treated endometrium, the top five up-regulated, fully annotated DEGs (DEGs with the highest log2FC values) were: Paired Box 6 (*PAX6*), Membrane Integral NOTCH2 Associated Receptor 1 (*MINAR1*), LY6/PLAUR Domain Containing 1 (*LYPD1*), Asparaginase (*ASPG*), Potassium Voltage-Gated Channel Modifier Subfamily S Member 2 (*KCNS2*). The top five

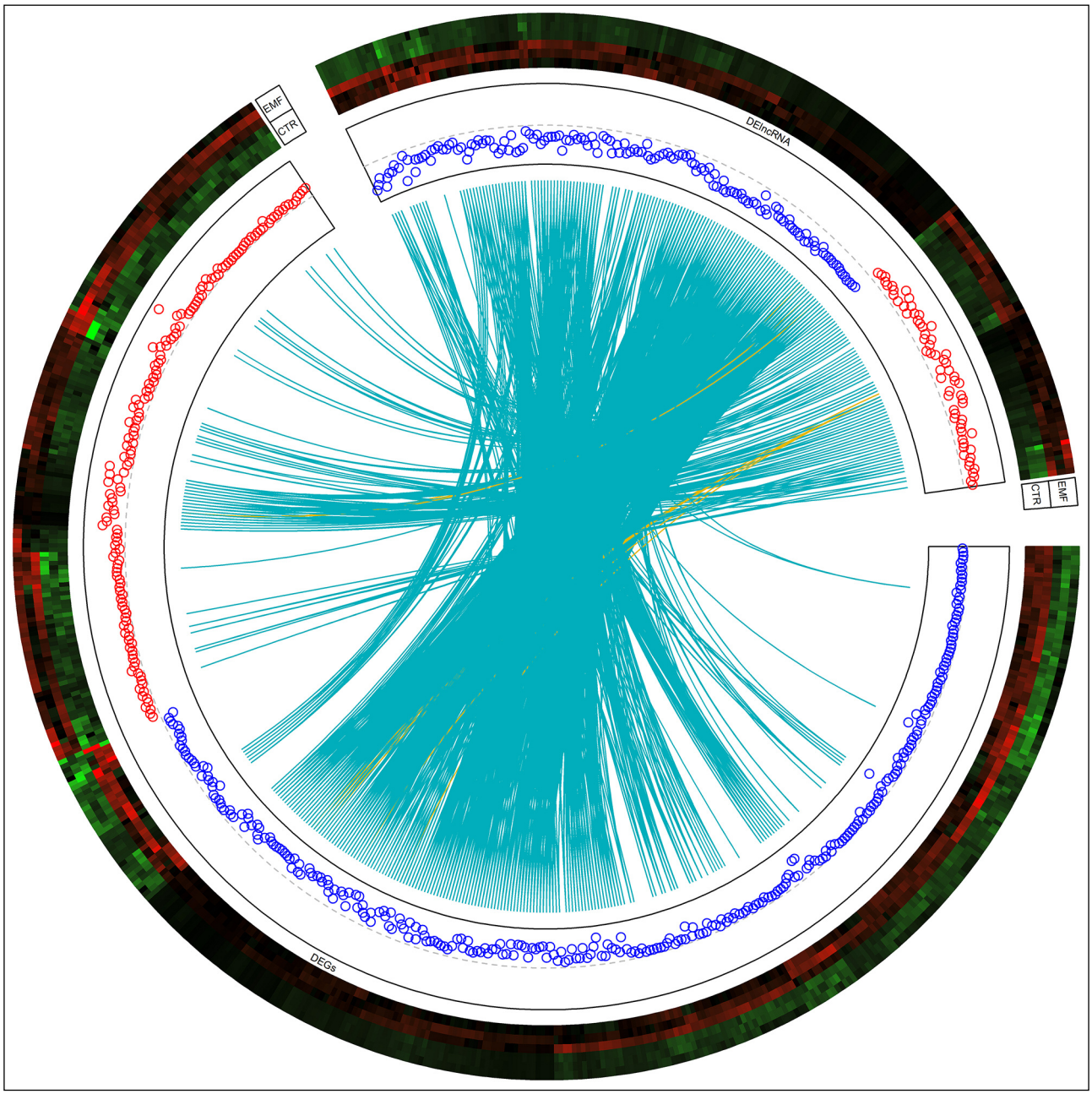

Fig. 2. Visualization of statistically significant changes (p-adjust < 0.05) in differentially expressed genes (DEGs) and long non-coding RNAs (DE-lncRNAs) under the influence of the electromagnetic field. The circle represents differentially expressed genes (DEGs, large part) and DE-lncRNAs (small part). Six upper tracks depict the normalized (Z-score; red-green scale) expression values for DEGs and DE-lncRNAs in each RNA-seq library. The circles in the next track describe increased (red) and decreased (blue) expression (logFC) in the compared groups. The following track presents the links between the correlated DEGs and DE-lncRNAs, where blue links depict positive correlations and yellow links denote negative correlations. The figure was generated with a circlize Bioconductor library and a custom R script.

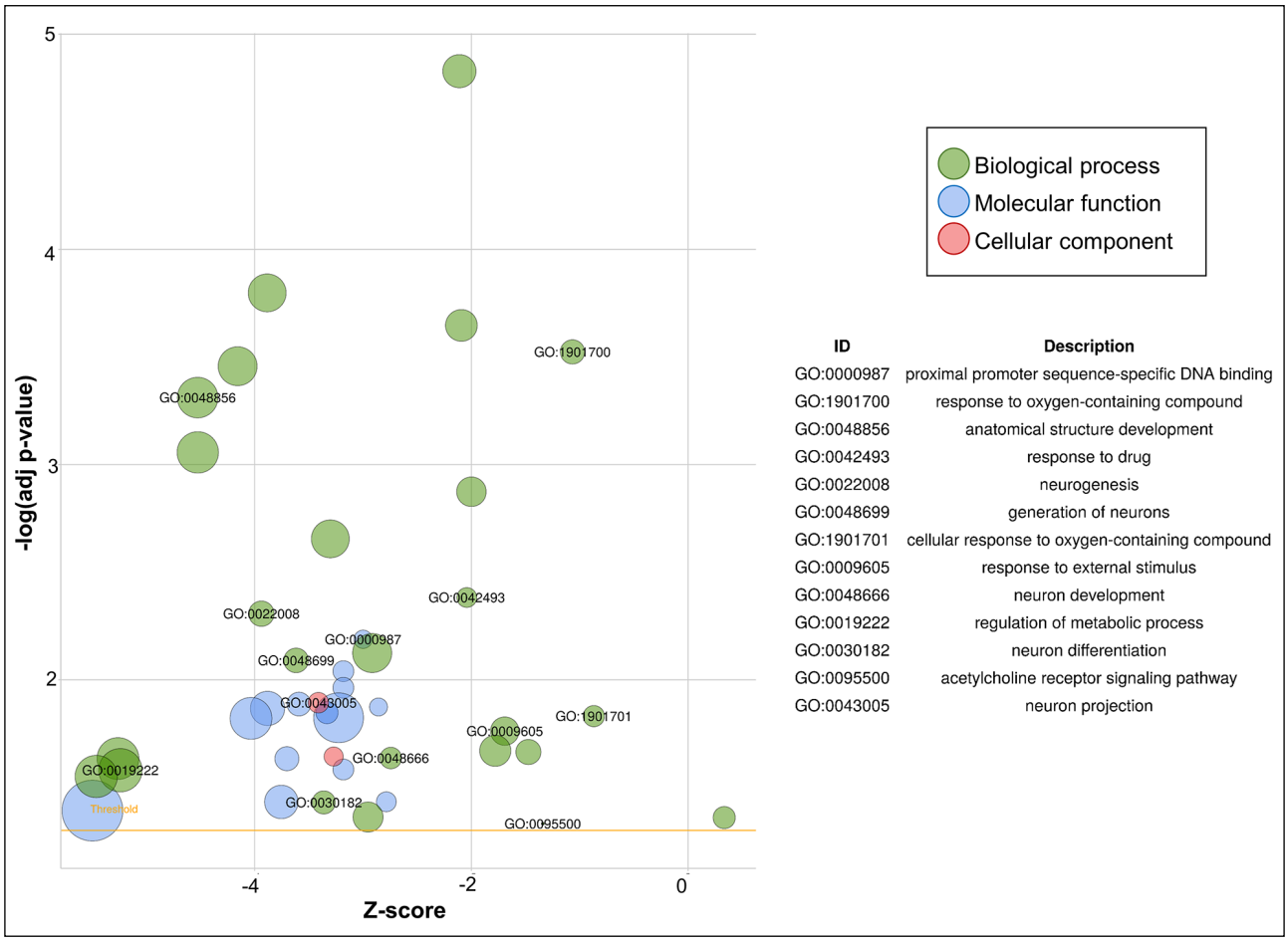

Fig. 3. Bubble chart of the ontology terms (biological process - green, cellular components - red, molecular function - blue) detected during a Gene Ontology (GO) analysis. Circle size refers to the logarithmic scale of adjusted *p*-value in the GO enrichment analysis. The X-axis describes the number of DEGs involved in enriched GO terms.

down-regulated, fully annotated DEGs (DEGs with the lowest log2FC values) were: Transcription Factor AP-2 Epsilon (*TFAP2E*), Retinal Degeneration 3, GUCY2D Regulator (*RD3*), Tripartite Motif Containing 69 (*TRIM69*), ELAV Like RNA Binding Protein 3 (*ELAVL3*), Epiphycan (*EPYC*). As a result of the filtration procedure (removal of one-exon transcripts, protein-coding genes, sequences with high coding potential, and short sequences) 210 transcripts identified as DE-lncRNAs were obtained from 1100 DE-ncRNAs (*Fig. 2*). Of those, 104 transcripts were classified in the ENSEMBL database. Other transcripts were novel and predicted in this study, and they included 148 down-regulated and 62 up-regulated transcripts (*Fig. 2*). A comparison of expression profiles revealed trans-interactions between 187 DE-lncRNAs and 207 target genes (absolute value of the Pearson correlation coefficient > 0.9).

Functional ontology annotations

A total of 341 DEGs were assigned to gene ontology annotations, and the results are visualized in *Fig. 3*. There were an estimated 15 GO annotations for molecular function (MF), 27 for biological process (BP), and 2 for cellular component (CC) terms. Eight of the identified GO BPs were related to cellular responses or metabolism, and five were linked with development. Two KEGG pathways were estimated: the apelin signaling pathway and parathyroid hormone synthesis, secretion, and action. A KEGG enrichment analysis revealed that the apelin signaling pathway was significantly enriched (adjusted *p*-value < 0.05), and that 8 genes (Adenylate Cyclase 8 - *ADCY8*, Adenylate Cyclase 10 - *ADCY10*, G Protein Subunit Alpha I1 - *GNAI1*, G Protein Subunit Alpha Q - *GNAQ*, G Protein Subunit Beta 5 - *GNB5*, Myocyte Enhancer Factor 2D - *MEF2D*, Protein Kinase C Epsilon - *PRKCE*, Ribosomal Protein S6 Kinase B1 - *RPS6KB1*) assigned to this enriched pathway were down-regulated, whereas 3 genes assigned to this enriched pathway were up-regulated (Nitric Oxide Synthase 3 - *NOS3*, Plasminogen Activator, Tissue Type - *PLAT*, Serpin Family E Member 1 - *SERPINE1*) (*Fig. 4*). The analysis also revealed that in the apelin signaling pathway, EMF treatment influenced the genes whose protein products are enzymes that participate in processes such as vasoconstriction, cell proliferation, cardiac hypertrophy, regulation of lipolysis in adipocytes, cardiovascular development, and inhibition of renal fibrosis. Some of these processes are related to angiogenesis.

RNA editing site prediction

The variant calling analysis revealed 247,983 SNVs in the EMF-treated endometrium. A total of 46,515 SNVs were eliminated from the downstream analysis using high-quality GATK filters. The porcine genome was screened to filter out 96,459 substitutions situated near bidirectional genes, paralogs, simple sequence repeats, and splice junction regions. An analysis of the variant calling frequency revealed 46,226 polymorphic sites with an alternative allele in at least half of RNA-seq libraries. A total of 2,563 substitutions annotated as single nucleotide polymorphisms (SNPs) with very high levels of alternative allele

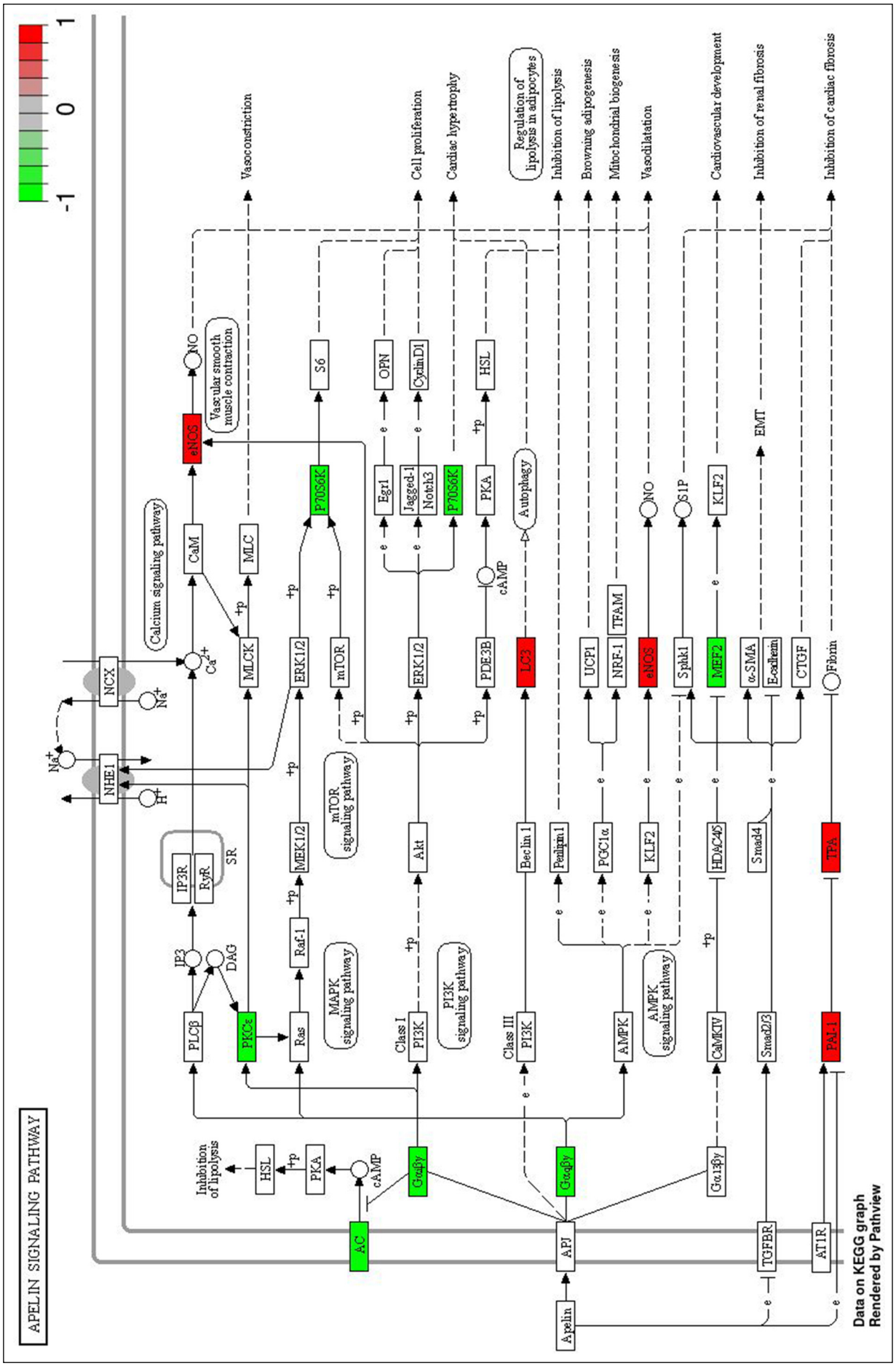

Fig. 4. KEGG (Kyoto Encyclopedia of Genes and Genomes) enrichment analysis of up-regulated and down-regulated differentially expressed genes (DEGs) that are involved in the apelin signaling pathway: *ADCY8* (*AC*), *ADCY10* (*AC*), *GNAI1* (*GaiBy*), *GNAQ* (*GaqBy*), *GNB5* (*GaqBy*), *MEF2D* (*MEF2*), *NOS3* (*eNOS*), *PLAT* (*TPA*), *PRKCE* (*PKCe*), *RPS6KB1* (*P70S6K*) and *SERPINE1* (*PAI-1*).

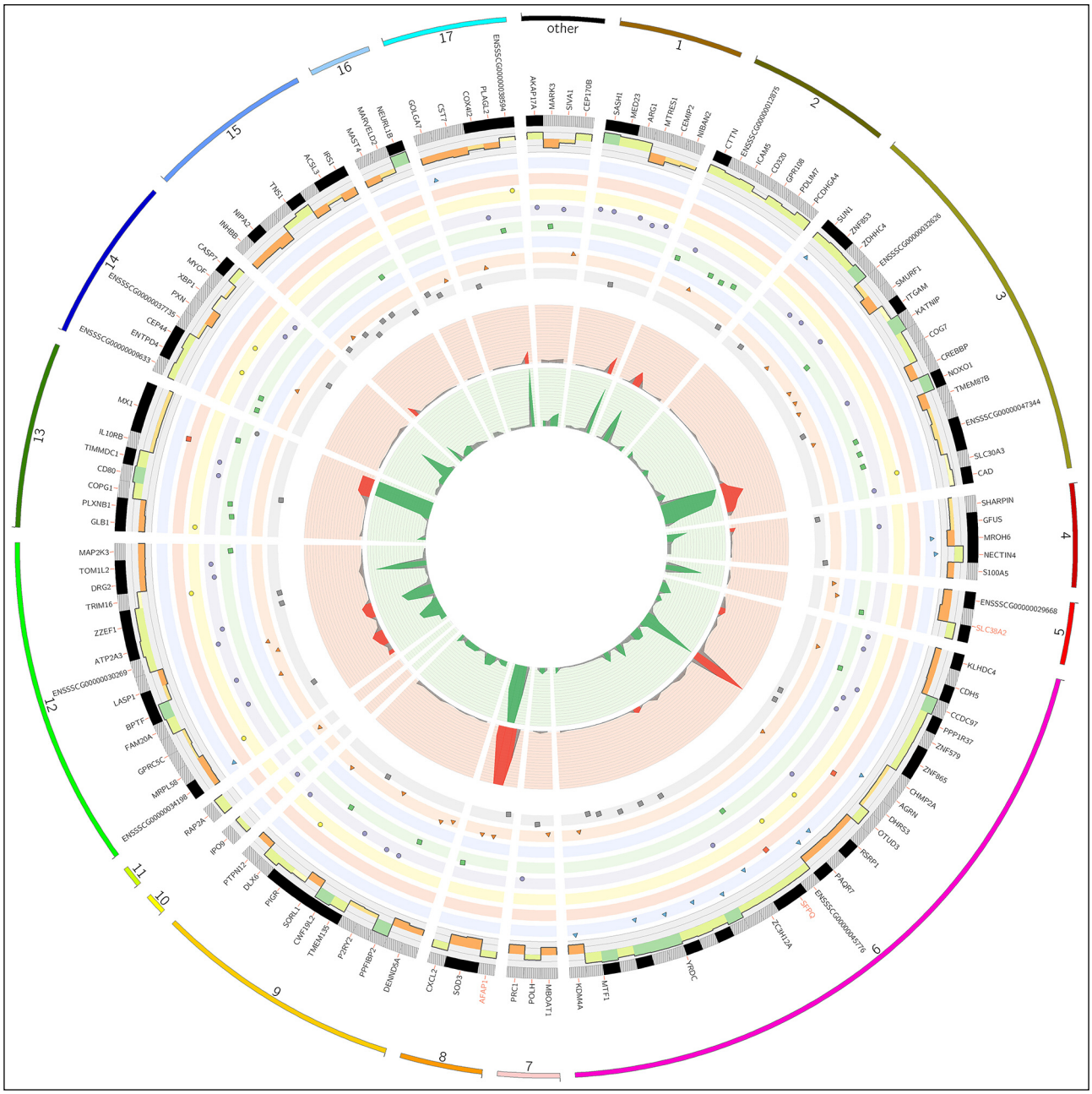

Fig. 5. Visualization of RNA editing candidates exposed to the electromagnetic field (EMF). The external circle represents porcine chromosomes and other unclassified scaffolds, where region length is proportional to the number of editing substitutions. The names of genes (differentially expressed genes DEGs are marked in red) identified in the vicinity of RNA candidates are placed outside the track. The second track (black and grey lined blocks) presents the types of RNA editing sites (adenine to inosine and cytosine to thymine, respectively). The third track (histogram) depicts differences in the alternative allele fraction (ΔAAF) between EMF-treated samples and the controls. The next eight middle scatter plots present the localization of RNA editing substitutions in upstream (blue triangles), 5'UTR (red rectangle), missense (yellow circle), synonymous (purple circle), intron (green squares), splice acceptor (grey circle), 3' UTR (orange triangle) and downstream (grey rectangle) regions. The two inner tracks show the coverage of alternative (red histogram) and reference variants (green histogram) in all RNA-seq libraries. The figure was generated with Circos software.

frequency (AAF > 0.7) were removed from every experimental sample. Next to the filtering procedure, 451 substitutions showed a significant (FDR < 0.001, *Δ*AAF > 0.1 and < –0.1) imbalance in the expression of alternate alleles between EMF-treated samples and the control. After the variant annotation procedure, 146 candidates were assigned as RNA canonical substitutions (adenine A to inosine I, and cytosine C to thymine T) in the transcriptome of the porcine endometrium (*Fig. 5*). The VEP assigned RNA editing candidates to the following groups of variants: 27 - 3'UTR, 3 - 5'UTR, 23 intronic, 1 - splice acceptor site, 38 - synonymous, 10 - missense, and 44 substitutions located in the vicinity of protein-coding genes (upstream or downstream region).

Validation of next-generation sequencing results

The DEGs in the endometrium exposed *in vitro* to EMF at the frequency of 50 Hz and the direction of changes (up- or down-regulated) were validated to confirm that the relative

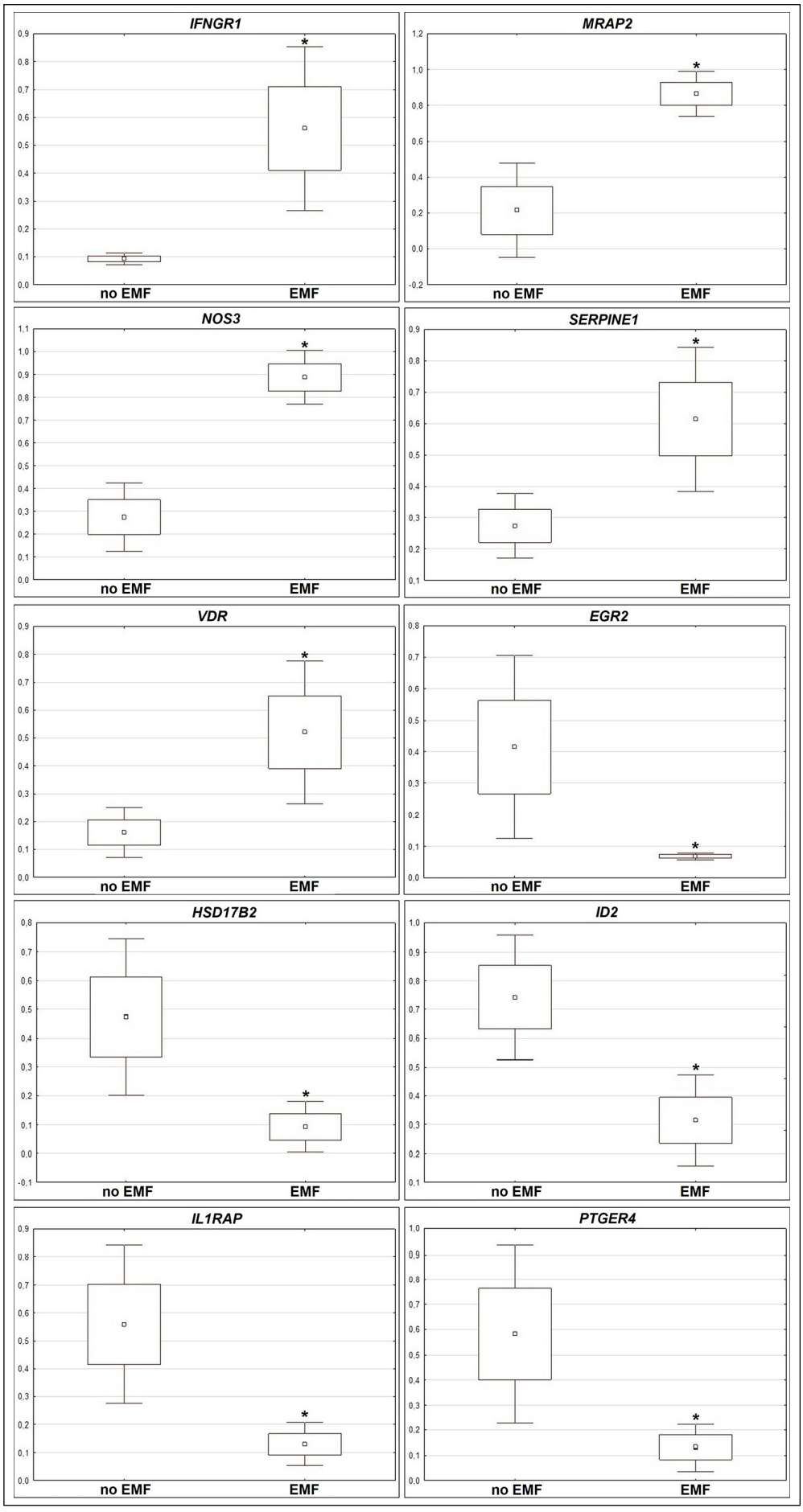

Fig. 6. Real-time PCR validation of RNA-seq results for differentially expressed genes DEGs in endometrial slices. The validation was performed for *EGR2*, *HSD17B2*, *ID2*, *IL1RAP*, *PTGER4* and *IFNGR1*, *MRAP2*, *NOS3*, *SERPINE1*, *VDR* genes vs. reference genes (*ACTB* and *GAPDH*). EMF, samples from electromagnetic field-treated groups; no EMF, samples from the control groups. Asterisk show the significant differences between control and EMF-treated samples ($p < 0.05$).

mRNA transcript abundance (Real-Time PCR) corresponds with the results of the NGS analysis. The validation procedure confirmed that Real-Time PCR and RNA-seq are consistent and of high quality. Up-regulated genes encoding *IFNGR1*, *MRAP2*, *NOS3*, *SERPINE1* and *VDR*, as well as down-regulated genes encoding *EGR2*, *HSD17B2*, *ID2*, *IL1RAP* and *PTGER4* were selected for the validation of transcriptome profiling results. The expression profiles of mRNAs encoded by the validated genes are presented in *Fig. 6*.

DISCUSSION

The results of this study demonstrated alterations in the transcriptomic profile of the endometrium treated *in vitro* with EMF at a frequency of 50 Hz for 2 h. A total of 1561 DE-TARs, including 1100 ncRNA and 461 DEGs, were identified. The vast majority of DEGs (66%) were down-regulated. This research also revealed that EMF treatment can evoke RNA editing events and influence the expression of endometrial transcripts. Exposure to EMF induced changes in 146 RNA editing sites in the genes expressed in the endometrium, and it could exert an impact on endometrial function. Three of the altered RNA editing variants were localized in vicinity of DEGs. SNVs may exert biological effects and may lead to the regulation of gene expression (45). In contrast, a previous study demonstrated that DEGs were mostly up-regulated in the porcine myometrium sampled during the peri-implantation period and exposed *in vitro* to EMF at a frequency of 50 Hz for 2 h (4). This observation could indicate that endometrial and myometrial tissues respond differently to EMF treatment, but both uterine tissues are sensitive to this external factor. The above indicates that EMF treatment can decrease the activity of some genes in the endometrium. It cannot be neglected that the physiological sensitivity of uterine tissues differs and mostly down-regulated endometrial transcriptomic response in the presence of EMF may be connected with the intrauterine hormonal environment created by the peri-implantation conceptuses which start to attach to the endometrial epithelial cells. However, these assumptions need further study.

In the present study, EMF treatment changed the abundance of endometrial mRNA transcripts that are important for endometrial function, including vitamin D receptor (*VDR*); hydroxysteroid 17(β) dehydrogenase 2 (*HSD17B2*); inhibitor of DNA binding 2 (*ID2*), interleukin 1 receptor accessory protein (*IL1RAP*); prostaglandin E receptor 4 (*PTGER4*); interferon-gamma receptor 1 (*IFNGR1*); melanocortin 2 receptor accessory protein 2 (*MRAP2*); early growth response 2 (*EGR2*); nitric oxide synthase 3 (*NOS3*); serpin family E member 1 (*SERPINE1*). The products of these genes are involved in the regulation of many processes in endometrial tissue, including proliferation (46-54).

The bioinformatic analysis revealed that *VDR* was up-regulated in the EMF-treated endometrium. According to the previous studies, the *VDR* mRNA transcript encoding VDR protein is involved in the regulation of uterine cell differentiation, calcium absorption that promotes bone development in fetuses, and steroidogenesis in the uterus (48, 55, 56). Vitamin D increases estrogen synthesis in the uterus *via* the vitamin D receptor (VDR) (55). Interestingly, the abundance of the *VDR* mRNA transcript was found to be higher in women with endometrial cancer (57), whereas the abundance of VDR protein was higher in women with ovarian cancer and cervical carcinomas (58). It was also indicated that platelet *VDR* content could be used as a pathological marker because this parameter was higher in women with ovarian cancer (59). This observation could suggest a correlation between VDR abundance and cancer. Increased abundance of the *VDR* mRNA transcript may influence cytokine levels or the local activity of immune cells, and it could play an important role in the prevalence and progression of endometriosis in humans (57). Moreover, the concentration of VDR protein in the endometrium was found to be higher in pregnant than in non-pregnant women (60), which suggests that VDR may play an important role during pregnancy. Therefore, by affecting *VDR* mRNA transcripts, EMF treatment may influence several processes associated with neoplasia, endometriosis and pregnancy success, and it can increase the levels of cytokine or immune cells (57-60).

Our results demonstrated that the *HSD17B2* mRNA transcript was down-regulated in the endometrium treated with EMF. The HSD17B2 enzyme acts as a regulator of steroid hormone metabolism, metabolizes estradiol-17β (E_2) to the less active estrone (E_1) and converts testosterone (T) to androstenedione (A_4) (46, 47). A previous study revealed that EMF treatment may decrease the secretion of A_4 in the endometrium (6). Respecting the knowledge on the role of vitamin D (55) and HSD17B2 (46) in the regulation of the steroidogenesis in the uterus, it can be assumed that by affecting *VDR* and *HSD17B2*, EMF influences estrogens and androgens sythesis and release by the endometrium, and contributes to changes in steroid hormone milieu in the uterus. As observed in the current study, EMF treatment increased the abundance of *VDR* and decreased the abundance of *HSD17B2* mRNA transcripts, thus contributing to excessive E_2 concentrations in the intrauterine environment. According to research, too high estrogen levels may exert cytotoxic effects on embryos during the peri-implantation period (61). For this reason, it cannot be ruled out that the EMF-related changes in *VDR* and *HSD17B2* mRNA transcript abundance could disrupt estrogen synthesis and metabolism in the endometrium.

The results of the current study also demonstrated that EMF treatment lowered the transcript abundance of *ID2* which is classified to GO:MF terms such as protein binding and DNA-binding transcription factor activity, as well as GO:BP terms such as developmental process, negative regulation of cellular process, negative regulation of biological process, response to external stimulus, and regulation of metabolic process. A recent study revealed that physiological *ID2* abundance in the porcine placenta is associated with the maintenance and regular course of pregnancy (50). It was also reported that embryo-derived interleukin-1β (IL1β) could decrease *ID2* transcript abundance in the endometrial slices of pigs during the implantation period (50). Our previous study provided evidence that IL1β is involved in the control of prostaglandin F2α (PGF2α) synthesis, release, and metabolism in the porcine endometrium to protect the corpus luteum during early pregnancy, which results in the production of prostaglandin E_2 (PGE_2) to overcome luteolysis (62, 63). The IL1β-mediated cell-signaling system is crucial for embryo-maternal interaction, which is important for the maintenance and establishment of pregnancy in pigs during the peri-implantation period (51). The results of the present study indicate that similarly to IL1β, EMF decreases *ID2* mRNA transcript abundance in the endometrium. This could disrupt implantation or lead to pregnancy loss. Additionally, it was found that the *ID2* mRNA transcript may be engaged in the migration of trophoblast cells (49, 50). In humans, disturbed expression of ID2 affects the proper cytotrophoblast development (49). It cannot be ruled out that by altering the expression of the *ID2* gene, EMF treatment may also contribute to the modulation of the endometrial structure.

In the present study, EMF lowered the expression of *IL1RAP*. During the rapid elongation of porcine conceptuses, required for the establishment of sufficient placental surface area for the transport of nutrients, porcine embryos are characterized

by a high abundance of the *IL1RAP* mRNA transcript (64). *IL1RAP* is needed for the activation of the IL1(*β*) cell-signaling pathway in the endometrium (51). As observed in the current study, decreased expression of *IL1RAP* in the EMF-treated endometrium may modulate the action of the IL1(*β*) cell-signaling system. During early pregnancy, the abundance of the *IL1RAP* mRNA transcript in the porcine endometrium is up-regulated by estrogens (65). It can be assumed that EMF may modify the activity of the IL1*β* cell-signaling system in the endometrium by altering the synthesis and release of estrogens in endometrial tissue. This observation suggests that by changing the secretion of endometrial estrogens, EMF may contribute to shaping the intrauterine environment during early pregnancy. It can be postulated that in pigs, lower endometrial expression of *IL1RAP* could influence the maintenance and establishment of pregnancy at the maternal-fetal line and, consequently, the EMF-induced changes in uterine estrogen levels could affect embryo development.

The results of the current study indicate that treatment with EMF decreased *PTGER4* transcript abundance in the endometrium. *PTGER4*, similarly to *ID2*, is classified to GO:BP terms such as negative regulation of cellular and biological process, and response to external stimulus. Waclawik *et al.* (66) found that the expression of the *PTGER4* mRNA transcript in the porcine endometrium was not altered by a female's reproductive status and no changes were visible during early pregnancy, but the abundance of PTGER4 protein was influenced by the day of pregnancy and was reduced on pregnancy day 15. *PTGER4* is very important during decidualization (67). Interestingly, unlike in humans, *PTGER4* mRNA transcript abundance is very low in bovine endometrial tissue (68). During the maternal recognition of pregnancy, *PTGER4* is not impacted by conceptus-derived factors (66). As observed in the current study, the disrupting effects of EMF may compromise endometrial *PTGER4* mRNA transcript abundance. Uterine tissues express PTGER4 which allows PGE_2 to express luteotropic and antiluteolytic properties that are necessary for pregnancy maintenance in pigs (23, 69-71). It is widely known that PGE_2 produced in the uterus acts in an autocrine/paracrine manner through PGE_2 receptors, resulting in the local increase of endometrial vascularization, angiogenesis, and enhanced uterine blood flow that supports implantation (23, 67, 70, 72). Thus, the results of the current study provide evidence that EMF treatment may disrupt important PGE_2-mediated changes in the uterus.

In the current study, EMF treatment increased the abundance of the *IFNGR1* mRNA transcript in the endometrium. Interferon-*γ* may play a crucial role in endometrial responsiveness to interferons (IFNs), which is essential for pregnancy establishment in pigs (73). According to Yoo *et al.* (73), the expression of interferon-*γ* receptors *IFNGR1* and *IFNGR2*, their regulation at the maternal-conceptus interface, and interferon signaling molecules could play a vital role in early pregnancy establishment in pigs. Interestingly, porcine trophoblast-derived IFNs stimulate the depolarization and remodeling of endometrial epithelial cells, and this process is essential for implantation and placenta development (74). Granulocytes, macrophages and lymphocytes occur in the stroma, and INFs may regulate endometrial function *via* stromal immune cells (75). There is evidence to suggest that IFNs stimulate *Mx*, *ISG15/17*, *IRF-1*, *STAT1* and *STAT2* mRNA transcript abundance in the endometrial stroma during early pregnancy (75, 76). It is important to note that the local intrauterine immune response plays an important role in pregnancy maintenance, and early-gravid female must accept a partially allogeneic embryo to ensure the survival of the fetus (77, 78). These observations suggest that by increasing the expression of *IFNGR1*, EMF may disrupt immune responses in the uterus, thus altering proper embryo development. Interestingly, EMF treatment of the myometrium also modulated immune-dependent processes associated with the regulation of *IFNA* signaling and interferon-alpha/beta signaling REACTOME pathways (4). It should also be emphasized that the EMF-induced increase in the abundance of the *IFNGR1* mRNA transcript in the endometrium may disrupt IFNs-mediated events in the pregnant uterus.

In the current study, EMF treatment increased *MRAP2* mRNA transcript abundance. D'Aurora *et al.* (79) reported that *MRAP2* was up-regulated in the endometrium of women with unexplained infertility and that increased expression of *MRAP2* mRNA influenced tissue stability. It cannot be ruled out that the EMF-related up-regulation of *MRAP2* in the endometrium may result in unexplained problems associated with endometrial receptivity during early pregnancy. An improved knowledge of the role played by *MRAP2* in the porcine endometrium during the peri-implantation period could broaden our understanding of the causes of female infertility. MRAP2 plays an important role in the control of energy homeostasis, and it is an endogenous inhibitor of orexin signaling (80). Orexin is an important regulatory factor that is produced locally in the uterus and affects uterine steroidogenesis (81) and the transcriptomic profile of the endometrium (82). In EMF-treated endometrium, the potential impact of orexin signaling on the over-expression of *MRAP2* could affect the genes that encode the synthesis of steroidogenic enzymes, secretion of steroid hormones, or the transcriptomic pattern of the porcine endometrium.

The results of the present study demonstrated that in the EMF-treated endometrium, the *EGR2* gene was down-regulated and classified to GO:BP terms such as system development, anatomical structure development, developmental process, regulation of multicellular organismal process, and response to external stimulus. This observation indicates that EMF may disrupt the mechanisms of endometrial development. The expression of *EGR2* was also down-regulated in the myometrium subjected to EMF treatment (4) with similar parameters to those described in the current study. EGR2 is essential for adipogenesis; it plays a crucial role in adipocyte differentiation, and changes in the abundance of the *EGR2* mRNA transcript may potentially impact the maintenance of energy homeostasis (83, 84). The EMF-altered expression of *MRAP2* and *EGR2*, genes that participate in the regulation of energy homeostasis, may influence reproductive functions which are linked with metabolic status. Research into uterine leiomyoma cells with knock-down of *EGR2* revealed a negative correlation with a higher cell proliferation rate (52). Lower *EGR2* expression in EMF-treated tissues may have the potential to disrupt cell proliferation. According to Song *et al.* (85), an increase in the proliferation of human cervical cancer HeLa and lung fibroblast IMR-90 cell lines is connected with the strength or exposure time to EMF. These observations suggest that by altering *EGR2* expression, EMF may also influence endometrial tissue proliferation in pigs, and thus contribute to implantation disorders.

Endometrial exposure to EMF increased the expression of *NOS3* which is classified to GO:BP terms such as system development, response to oxygen-containing compound, multicellular organism development, anatomical structure development, developmental process, negative regulation of cellular process, negative regulation of biological process, cellular response to oxygen-containing compound, response to external stimulus, and regulation of multicellular organismal process. Thus, by altering *NOS3* expression, EMF may disrupt the physiological processes related to development, process regulation, or responses to external factors that induce oxidative stress. Oxidative stress is an imbalance between the production and accumulation of reactive oxygen species in tissues. Increased production of reactive oxygen species may lead to imbalance and

damage of cells or tissues (86). Free radicals are produced from both endogenous and exogenous sources. They are generated as by-products in response to metabolized or degraded compounds, and they affect the entire organism and may cause infection, cancer, stress or aging processes (86). Nitric oxide radicals are formed when arginine is oxidized to citrulline by nitric oxide synthase (NOS) (86), and they have the potential to damage DNA (87). The EMF-induced increase in the abundance of the *NOS3* mRNA transcript a could disrupt the processes mediated by nitric oxide radicals. A study conducted on mice revealed that oxidative stress may emerge in the tissues of mothers and their offspring who were exposed to EMF treatment during pregnancy (88). Ota *et al.* (53) suggested that higher expression of endothelial NOS in the human endometrium plays a role in endometriosis. Higher expression of NOS can be associated with the proliferative effects of estrogen, which indicates that NOS may affect uterine function and lead to changes in blood flow (89). It should be emphasized that normal uteroplacental blood flow is crucial for embryo development and normal birth weight (90). Therefore, it is possible that by influencing *NOS3* expression, EMF may impact uterine blood flow and thus affect endometrial stability.

EMF treatment results in the up-regulation of *SERPINE1* mRNA transcripts in the exposed endometrium. EMF-induced *SERPINE1* is classified to GO:BP terms associated with, among others, developmental processes, and it is involved in the apelin signaling pathway. *SERPINE1* plays a crucial role by exhibiting conformational and functional properties, affecting cell migration, and modulating the risk of cardiovascular diseases and tumor development (54). In the porcine oviduct, SERPINE1 is expressed in the presence of spermatozoa and embryos, and it can prevent early implantation of embryos with invasive potential (91, 92). An increase in SERPINE1 protein accompanying decidualization and further over-expression of SERPINE1 may pathologically inhibit trophoblast invasion (93). In the present study, the EMF-induced increase in *SERPINE1* mRNA transcript abundance could inhibit trophoblast invasion. The above may suggest that EMF treatment leads to the over-expression of *SERPINE1* in the endometrium, thus influencing the processes responsible for uterine activity, by modulating cell migration and disrupting fertilization or embryo development.

The results of the current study indicate that *NOS3* and *SERPINE1*, which were up-regulated as a result of EMF treatment, are located in the apelin signaling pathway (KEGG). In the endometrial tissue treated with EMF, the apelin signaling pathway was the most representative subcategory based on an analysis of the KEGG database. The apelin/APJ system might be engaged in the cardiovascular system, adipose tissue, obesity-associated disorders (94) or physiological functions by regulating the size-sensing mechanism of blood vessels (95), and it can be a marker of oxidative stress during pregnancy (96). The above could indicate that EMF treatment may regulate endometrial function or lead to endometrial instability by changing the expression of *NOS3* and *SERPINE1* in the tissue.

It cannot be ruled out that exposure to EMF deregulates the expression of genes encoding proteins that are involved in crucial biological processes during the peri-implantation period. The present study demonstrated that *VDR*, *ID2*, *NOS3* and *SERPINE1* genes were involved in negative regulation of biological process and regulation of metabolic process. Altered expression of genes influencing biological and metabolic processes may affect the intrauterine environment needed for embryo development. In reference to the existing knowledge about the consequences of EMF treatment, this study focused on the possible mechanisms that can be regulated or changed through EMF treatment in the porcine endometrium during the unique peri-implantation period.

In conclusion, EMF treatment alters the transcriptomic profile of the endometrium. The observed changes in mRNA transcript abundance affect the regulation of estrogen synthesis and metabolism, endometrial structure, maintenance and establishment of pregnancy at the maternal-fetal line, and they disrupt IFNs-mediated events. Moreover, EMF treatment impacts orexin signaling; it is involved in the regulation of energy homeostasis; it may influence metabolic status, endometrial tissue proliferation and uterine blood flow, and it may modulate cell migration and cause endometrial instability. Special attention should be given to the consequences of short-term (2 h) EMF treatment at an extremely low frequency of 50 Hz. The presented results provide valuable inputs for future studies exploring the mechanism of EMF treatment on the reproductive system.

Authors' contributions: Conceptualization, A.F. and E.M.D.; acquisition of data, W.K. and E.M.D.; data curation, W.K. and L.P.; formal analysis, W.K., E.M.D. and L.P.; funding acquisition, A.F.; investigation, W.K., E.M.D. and L.P.; methodology, E.M.D., A.F. and W.K.; project administration, A.F.; resources, W.K., E.M.D. and A.F.; software, W.K., L.P. and J.P.J.; supervision, A.F.; validation, L.P., A.Z. and A.F.; visualization, W.K., L.P. and J.P.J.; writing - original draft, W.K.; interpretation of data and conclusions, W.K.; writing -review and editing, W.K., E.M.D., L.P., A.Z., P.J.W. and A.F. All authors have read and agreed to the published version of the manuscript.

Data availability statement: The raw data used for the preparation of the presented results are available in the European Nucleotide Archive (ENA) under accession No. PRJEB50034.

Suplementary tables are avilable online: https://doi.org/10.7910/DVN/KVDUIB:

Supplementary Table 1. Differentially expressed transcriptional active regions (DE-TARs) were identified after EMF treatment at 50 Hz for 2 h. DE-TARs were divided into genes (DEGs), long noncoding RNAs (DElncRNAs) and other noncoding transcripts.

Supplementary Table 2. GO terms and KEGG and HP pathways evaluated in the endometrium exposed to EMF at 50 Hz for 2 h.

Supplementary Table 3. Potential RNA editing sites were identified in the experiment. The RNA editing candidates were evaluated based on differences in allele frequency between EMF-treated endometrial slices and control groups.

Funding: This research was funded by the National Science Centre, Poland – OPUS grant number: 2017/25/B/NZ9/00090. Wiktoria Kozlowska is a recipient of a scholarship from the Programme Interdisciplinary Doctoral Studies in Biology and Biotechnology (POWR.03.05.00-00-Z310/17) which is funded by the European Social Fund, "Development Program of the University of Warmia and Mazury in Olsztyn" (POWR.03.05.00-00-Z310/17), co-financed by the European Union under the European Social Fund from the Operational Program Knowledge Education Development.

Acknowledgments: The authors would like to thank Professor Anna Koziorowska (College of Natural Sciences, University of Rzeszow, Poland) for assistance in designing the EMF treatment protocol.

Conflicts of interest: None declared.

REFERENCES

1. Mansuori E, Alihemmati A, Mesbahi A. An overview on the effects of power frequency electromagnetic field exposure

on the female reproduction system, pregnancy outcome and fetal development. *J Med Chem Sci* 2020; 3: 60-70.
2. Gajsek P, Ravazzani P, Grellier J, Samaras T, Bakos J, Thuroczy G. Review of studies concerning electromagnetic field (EMF) exposure assessment in Europe: low frequency fields (50 Hz-100 kHz). *Int J Environ Res Public Health* 2016; 13: 875. doi: 10.3390/ijerph13090875
3. Ahuja YR, Vijayashree B, Saran R, Jayashri EL, Manoranjani JK, Bhargava SC. In vitro effects of low-level, low-frequency electromagnetic fields on DNA damage in human leucocytes by comet assay. *Indian J Biochem Biophys* 1999; 36: 318-322.
4. Drzewiecka EM, Kozlowska W, Paukszto L, *et al.* Effect of the electromagnetic field (EMF) radiation on transcriptomic profile of pig myometrium during the peri-implantation period - an in vitro study. *Int J Mol Sci* 2021; 22: 7322. doi: 10.3390/ijms22147322
5. Drzewiecka EM, Kozlowska W, Zmijewska A, Wydorski PJ, Franczak A. Electromagnetic field (EMF) radiation alters estrogen release from the pig myometrium during the peri-implantation period. *Int J Mol Sci* 2021; 22: 2920. doi: 10.3390/ijms22062920
6. Kozlowska W, Drzewiecka EM, Zmijewska A, Koziorowska A, Franczak A. Effects of electromagnetic field (EMF) radiation on androgen synthesis and release from the pig endometrium during the fetal peri-implantation period. *Anim Reprod Sci* 2021; 226: 106694. doi: 10.1016/j.anireprosci.2021.106694
7. Mahaki H, Jabarivasal N, Sardanian K, Zamani A. Effects of various densities of 50 Hz electromagnetic field on serum IL-9, IL-10, and TNF-α levels. *Int J Occup Env Med* 2020; 11: 24-32.
8. Svedenstal BM, Johanson KJ, Mild KH. DNA damage induced in brain cells of CBA nice exposed to magnetic fields. *In Vivo* 1999; 13: 551-552.
9. Chow KC, Tung WL. Magnetic field exposure enhances DNA repair through the induction of DnaK/J synthesis. *FEBS Lett* 2000; 478: 133-136.
10. Lourencini Da Silva R, Albano F, Lopes Dos Santos LR, Tavares AD, Felzenszwalb I. The effect of electromagnetic field exposure on the formation of DNA lesions. *Redox Rep* 2000; 5: 299-301.
11. Robison JG, Pendleton AR, Monson KO, Murray BK, O'Neill KL. Decreased DNA repair rates and protection from heat induced apoptosis mediated by electromagnetic field exposure. *Bioelectromagnetics* 2002; 23: 106-112.
12. Schmitz C, Keller E, Freuding T, Silny J, Korr H. 50-Hz magnetic field exposure influences DNA repair and mitochondrial DNA synthesis of distinct cell types in brain and kidney of adult mice. *Acta Neuropathol* 2004; 107: 257-264.
13. Gye MC, Park CJ. Effect of electromagnetic field exposure on the reproductive system. *Clin Exp Reprod Med* 2012; 39: 1-9. doi: 10.5653/cerm.2012.39.1.1
14. Koziorowska A, Waszkiewicz EM, Romerowicz-Misielak M, Zglejc-Waszak K, Franczak A. Extremely low-frequency electromagnetic field (EMF) generates alterations in the synthesis and secretion of oestradiol-17β (E2) in uterine tissues: an in vitro study. *Theriogenology* 2018; 1: 86-95.
15. Franczak A, Waszkiewicz E, Kozlowska W, Zmijewska A, Koziorowska A. Consequences of electromagnetic field (EMF) radiation during early pregnancy - androgen synthesis and release from the myometrium of pigs in vitro. *Anim Reprod Sci* 2020; 218: 106465. doi: 10.1016/j.anireprosci.2020.106465
16. Darwish SM, Darwish A, Darwish DS. An extremely low-frequency magnetic field can affect CREB protein conformation which may have a role in neuronal activities including memory. *J Phys Commun* 2020; 4: 1-10. doi: 10.1088/2399-6528/ab66d2
17. Karimi A, Moghaddam FG, Valipour M. Insights in the biology of extremely low-frequency magnetic fields exposure on human health. *Mol Biol Rep* 2020; 47: 5621-5633.
18. Spencer TE, Johnson GA, Burghardt RC, Bazer FW. Progesterone and placental hormone actions on the uterus: insights from domestic animals. *Biol Reprod* 2004; 71: 2-10. doi: 10.1095/biolreprod.103.024133
19. Ataman MB, Akoz M, Mustafa KS, Erdem H, Bucak MN. Prevention of embryonic death using different hormonal treatments in ewes. *Turkish J Vet Anim Sci* 2013; 37: 6-8.
20. Jarvis GE. Early embryo mortality in natural human reproduction: what the data say. *F1000Research* 2017; 5: 2765. doi: 10.12688/f1000research.8937.2
21. Geisert RD, Zavy MT, Moffatt RJ, Blair RM, Yellin T. Embryonic steroids and the establishment of pregnancy in pigs. *J Reprod Fertil Suppl* 1990; 40: 293-305.
22. Ziecik AJ, Blitek A, Kaczmarek MM, Waclawik A, Bogacki M. Inhibition of luteolysis and embryo-uterine interactions during the peri-implantation period in pigs. *Soc Reprod Fertil Suppl* 2006; 62: 147-161.
23. Waclawik A, Kaczmarek MM, Blitek A, Kaczynski P, Ziecik AJ. Embryo-maternal dialogue during pregnancy establishment and implantation in the pig. *Mol Reprod Dev* 2017; 84: 842-855.
24. Gellersen B, Brosens JJ. Cyclic decidualization of the human endometrium in reproductive health and failure. *Endocr Rev* 2014; 35: 851-905.
25. Cermisoni GC, Alteri A, Corti L, *et al.* Vitamin D and endometrium: a systematic review of a neglected area of research. *Int J Mol Sci* 2018; 19: 2320. doi: 10.3390/ijms19082320
26. Paukszto L, Mikolajczyk A, Szeszko K, Smolinska N, Jastrzebski JP, Kaminski T. Transcription analysis of the response of the porcine adrenal cortex to a single subclinical dose of lipopolysaccharide from Salmonella Enteritidis. *Int J Biol Macromol* 2019; 141: 1228-1245.
27. Andrews S. FastQC. A Quality Control Tool for High Throughput Sequence Data. *Babraham Bioinforma*. Available online http//www.bioinformatics.babraham.ac.uk /projects/fastqc (accessed 1 January 2020) 2010
28. Bolger AM, Lohse M, Usadel B. Trimmomatic: a flexible trimmer for Illumina sequence data. *Bioinformatics* 2014; 30: 2114-2120.
29. Dobin A, Davis CA, Schlesinger F, *et al.* STAR: ultrafast universal RNA-seq aligner. *Bioinformatics* 2013; 29: 15-21.
30. Pertea M, Pertea GM, Antonescu CM, Chang TC, Mendell JT, Salzberg SL. StringTie enables improved reconstruction of a transcriptome from RNA-seq reads. *Nat Biotechnol* 2015; 33: 290-295.
31. Robinson MD, McCarthy DJ, Smyth GK. edgeR: a bioconductor package for differential expression analysis of digital gene expression data. *Bioinformatics* 2010; 26: 139-140.
32. Love MI, Huber W, Anders S. Moderated estimation of fold change and dispersion for RNA-seq data with DESeq2. *Genome Biol* 2014; 15: 550. doi: 10.1186/s13059-014-0550-8
33. Kanehisa M, Furumichi M, Sato Y, Ishiguro-Watanabe M, Tanabe M. KEGG: integrating viruses and cellular organisms. *Nucleic Acids Res* 2021; 49: 545-551.
34. Kanehisa M. Toward understanding the origin and evolution of cellular organisms. *Protein Sci* 2019; 28: 1947-1951.
35. Kanehisa M, Goto S. KEGG: kyoto encyclopedia of genes and genomes. *Nucleic Acids Res* 2000; 28: 27-30.

36. Reimand J, Arak T, Adler P, *et al.* Profiler-a web server for functional interpretation of gene lists. *Nucleic Acids Res* 2016; 44: W83-W89.
37. Wang L, Park HJ, Dasari S, Wang S, Kocher JP, Li W. CPAT: coding-potential assessment tool using an alignment-free logistic regression model. *Nucleic Acids Res* 2013; 41: e74. doi: 10.1093/nar/gkt006
38. Li A, Zhang J, Zhou Z. PLEK: a tool for predicting long non-coding RNAs and messenger RNAs based on an improved k-mer scheme. *BMC Bioinformatics* 2014; 15: 311. doi: 10.1186/1471-2105-15-311
39. Kang YJ, Yang DC, Kong L, *et al.* CPC2: a fast and accurate coding potential calculator based on sequence intrinsic features. *Nucleic Acids Res* 2017; 45: 12-16.
40. Wang J, Pan Y, Shen S, Lin L, Xing Y. rMATS-DVR: rMATS discovery of differential variants in RNA. *Bioinformatics* 2017; 33: 2216-2217.
41. McKenna A, Hanna M, Banks E, *et al.* The Genome Analysis Toolkit: a MapReduce framework for analyzing next-generation DNA sequencing data. *Genome Res* 2010; 20: 1297-1303.
42. McLaren W, Gil L, Hunt SE, *et al.* The Ensembl Variant Effect Predictor. *Genome Biol* 2016; 17: 122. doi: 10.1186/s13059-016-0974-4
43. Krzywinski M, Schein J, Birol I, *et al.* Circos: an information aesthetic for comparative genomics. *Genome Res* 2009; 19: 1639-1645.
44. Bustin SA, Benes V, Garson JA, *et al.* The MIQE guidelines: minimum information for publication of quantitative real-time PCR experiments. *Clin Chem* 2009; 55: 611-622.
45. Spencer DH, Zhang B, Pfeifer J. Single nucleotide variant detection using next generation sequencing. In: Clinical Genomics 2015, pp. 109-127.
46. Mindnich R, Moller G, Adamski J. The role of 17 beta-hydroxysteroid dehydrogenases. *Mol Cell Endocrinol* 2004; 218: 7-20.
47. Moeller G, Adamski J. Multifunctionality of human 17β-hydroxysteroid dehydrogenases. *Mol Cell Endocrinol* 2006; 248: 47-55.
48. Yoshizawa T, Handa Y, Uematsu Y, *et al.* Mice lacking the vitamin D receptor exhibit impaired bone formation, uterine hypoplasia and growth retardation after weaning. *Nat Genet* 1997; 16: 391-396.
49. Janatpour MJ, McMaster MT, Genbacev O, *et al.* Id-2 regulates critical aspects of human cytotrophoblast differentiation, invasion and migration. *Development* 2000; 127: 549-558.
50. Han J, Seo H, Choi Y, *et al.* Expression and regulation of inhibitor of DNA binding proteins ID1, ID2, ID3, and ID4 at the maternal-conceptus interface in pigs. *Theriogenology* 2018; 108: 46-55.
51. Seo H, Choi Y, Shim J, Choi Y, Ka H. Regulatory mechanism for expression of IL1B receptors in the uterine endometrium and effects of IL1B on prostaglandin synthetic enzymes during the implantation period in pigs. *Biol Reprod* 2012; 87: 31-32.
52. Yin P, Navarro A, Fang F, *et al.* Early growth response-2 expression in uterine leiomyoma cells: regulation and function. *Fertil Steril* 2011; 96: 439-444.
53. Ota H, Igarashi S, Hatazawa J, Tanaka T. Endothelial nitric oxide synthase in the endometrium during the menstrual cycle in patients with endometriosis and adenomyosis. *Fertil Steril* 1998; 69: 303-308.
54. Gils A, Declerck P. Plasminogen activator inhibitor-1. *Curr Med Chem* 2004; 11: 2323-2334.
55. Grzesiak M, Waszkiewicz E, Wojtas M, Kowalik K, Franczak A. Expression of vitamin D receptor in the porcine uterus and effect of 1,25(OH)2D3 on progesterone and estradiol-17β secretion by uterine tissues in vitro. *Theriogenology* 2019; 125: 102-108.
56. Zhang L, Hu J, Li M, Shang Q, Liu S, Piao X. Maternal 25-hydroxycholecalciferol during lactation improves intestinal calcium absorption and bone properties in sow-suckling piglet pairs. *J Bone Miner Metab* 2019; 37: 1083-1094.
57. Agic A, Xu H, Altgassen C, *et al.* Relative expression of 1,25-dihydroxyvitamin D3 receptor, vitamin D 1α-hydroxylase, vitamin D 24-hydroxylase, and vitamin D 25-hydroxylase in endometriosis and gynecologic cancers. *Reprod Sci* 2007; 14: 486-497.
58. Friedrich M, Rafi L, Mitschele T, Tilgen W, Schmidt W, Reichrath J. Analysis of the vitamin D system in cervical carcinomas, breast cancer and ovarian cancer. *Recent Results Cancer Res* 2003; 164: 239-246.
59. Silvagno F, Poma BP, Realmuto C, *et al.* Analysis of vitamin D receptor expression and clinical correlations in patients with ovarian cancer. *Gynecol Oncol* 2010; 119: 121-124.
60. Guo J, Liu S, Wang P, Ren H, Li Y. Characterization of VDR and CYP27B1 expression in the endometrium during the menstrual cycle before embryo transfer: implications for endometrial receptivity. *Reprod Biol Endocrinol* 2020; 18: 24. doi: 10.1186/s12958-020-00579-y
61. Geisert RD, Ross JW, Ashworth MD, White FJ, Johnson GA, DeSilva U. Maternal recognition of pregnancy signal or endocrine disruptor: the two faces of oestrogen during establishment of pregnancy in the pig. *Soc Reprod Fertil Suppl* 2006; 62: 131-145.
62. Franczak A, Zmijewska A, Kurowicka B, Wojciechowicz B, Petroff BK, Kotwica G. The effect of tumor necrosis factor α (TNFα), interleukin 1β (IL1β) and interleukin 6 (IL6) on endometrial PGF 2α synthesis, metabolism and release in early-pregnant pigs. *Theriogenology* 2012; 77: 155-165.
63. Franczak A, Zmijewska A, Kurowicka, B Wojciechowicz B, Kotwica G. Interleukin 1β-induced synthesis and secretion of prostaglandin E_2 in the porcine uterus during various periods of pregnancy and the estrous cycle. *J Physiol Pharmacol* 2010; 61: 733-742.
64. Mathew DJ, Lucy MC, Geisert RD. Interleukins, interferons, and establishment of pregnancy in pigs. *Reproduction* 2016; 151: 111-122.
65. Seo H, Kim M, Choi Y, Choi Y, Ka H. Expression and regulation of IL1B receptor subtypes, IL1R1 and IL1RAP, in the uterine endometrium during pregnancy in pigs. *Biol Reprod* 2011; 85: 484-484.
66. Waclawik A, Jabbour HN, Blitek A, Ziecik AJ. Estradiol-17beta, prostaglandin E2 (PGE2), and the PGE2 receptor are involved in PGE2 positive feedback loop in the porcine endometrium. *Endocrinology* 2009; 150: 3823-3832.
67. Kennedy TG, Gillio-Meina C, Phang SH. Prostaglandins and the initiation of blastocyst implantation and decidualization. *Reproduction* 2007;134: 635-643.
68. Arosh JA, Banu SK, Chapdelaine P, *et al.* Molecular cloning and characterization of bovine prostaglandin E2 receptors EP2 and EP4: expression and regulation in endometrium and myometrium during the estrous cycle and early pregnancy. *Endocrinology* 2003; 144: 3076-3091.
69. Waclawik A, Kaczynski P, Jabbour HN. Autocrine and paracrine mechanisms of prostaglandin E2 action on trophoblast/conceptus cells through the prostaglandin E2 receptor (PTGER2) during implantation. *Endocrinology* 2013; 154: 3864-3876.
70. Christenson LK, Anderson LH, Ford SP, Farley DB. Luteal maintenance during early pregnancy in the pig: role for prostaglandin E2. *Prostaglandins* 1994; 47: 61-75.

71. Ziecik AJ. Old, new and the newest concepts of inhibition of luteolysis during early pregnancy in pig. *Domest Anim Endocrinol* 2002; 23: 265-275.
72. Hamilton GS, Kennedy TG. Uterine vascular changes after unilateral intrauterine infusion of indomethacin and prostaglandin E2 to rats sensitized for the decidual cell reaction. *Biol Reprod* 1994; 50: 757-764.
73. Yoo I, Seo H, Choi Y, *et al.* Analysis of interferon-γ receptor IFNGR1 and IFNGR2 expression and regulation at the maternal-conceptus interface and the role of interferon-γ on endometrial expression of interferon signaling molecules during early pregnancy in pigs. *Mol Reprod Dev* 2019; 86: 1993-2004.
74. Cencic A, Guillomot M, Koren S, La Bonnardiere C. Trophoblastic interferons: do they modulate uterine cellular markers at the time of conceptus attachment in the pig? *Placenta* 2003; 24: 862-869.
75. Spencer TE, Bazer FW. Conceptus signals for establishing and maintenance of pregnancy. *Reprod Biol Endocrinol* 2004; 2: 49. doi: 10.1186/1477-7827-2-49
76. Hicks BA, Etter SJ, Carnahan KG, *et al.* Expression of the uterine Mx protein in cyclic and pregnant cows, gilts, and mares. *J Anim Sci* 2003; 81: 1552-1561.
77. van Nieuwenhoven ALV, Heineman MJ, Faas MM. The immunology of successful pregnancy. *Hum Reprod Update* 2003; 9: 347-357.
78. Poole JA, Claman HN. Immunology of pregnancy. *Clin Rev Allergy Immunol* 2004; 26: 161-170.
79. D'Aurora M, Romani F, Franchi S, *et al.* MRAP2 regulates endometrial receptivity and function. *Gene* 2019; 703: 7-12.
80. Rouault AAJ, Lee AA, Sebag JA. Regions of MRAP2 required for the inhibition of orexin and prokineticin receptor signaling. *Biochim Biophys Acta* 2017; 1864: 2322-2329.
81. Rytelewska E, Kisielewska K, Gudelska M, *et al.* The effect of orexin a on the StAR, CYP11A1 and HSD3B1 gene expression, as well as progesterone and androstenedione secretion in the porcine uterus during early pregnancy and the oestrous cycle. *Theriogenology* 2020; 143: 179-190.
82. Dobrzyn K, Szeszko K, Kiezun M, *et al.* In vitro effect of orexin A on the transcriptomic profile of the endometrium during early pregnancy in pigs. *Anim Reprod Sci* 2019; 200: 31-42.
83. Chen Z, Torrens JI, Anand A, Spiegelman BM, Friedman JM. Krox20 stimulates adipogenesis via C/EBPβ-dependent and independent mechanisms. *Cell Metab* 2005; 1: 93-106.
84. Boyle KB, Hadaschik D, Virtue S, *et al.* The transcription factors Egr1 and Egr2 have opposing influences on adipocyte differentiation. *Cell Death Differ* 2009; 16: 782-789.
85. Song K, Im SH, Yoon YJ, Kim HM, Lee HJ, Park GS. A 60 Hz uniform electromagnetic field promotes human cell proliferation by decreasing intracellular reactive oxygen species levels. *PLoS One* 2018; 13: e0199753. doi: 10.1371/journal.pone.0199753
86. Pizzino G, Irrera N, Cucinotta M, *et al.* Oxidative stress: harms and benefits for human health. *Oxid Med Cell Longev* 2017; 2017: 8416763. doi: 10.1155/2017/8416763
87. Valko M, Izakovic M, Mazur M, Rhodes CJ, Telser J. Role of oxygen radicals in DNA damage and cancer incidence. *Mol Cell Biochem* 2004; 266: 37-56.
88. Toossi MH, Sadeghnia HR, Feyzabadi MM, *et al.* Exposure to mobile phone (900-1800 MHz) during pregnancy: tissue oxidative stress after childbirth. *J Matern Neonatal Med* 2018; 31: 1298-1303.
89. Khorram O, Garthwaite M, Magness RR. Endometrial and myometrial expression of nitric oxide synthase isoforms in pre- and postmenopausal women. *J Clin Endocrinol Metab* 1999; 84: 2226-2232.
90. Magness RR. Maternal cardiovascular and other physiologic responses to the endocrinology of pregnancy. In: Endocrinology of Pregnancy. Bazer FW (ed.) *Humana Press* 1998, pp. 507-539.
91. Kouba AJ, Alvarez IM, Buhi WC. Identification and localization of plasminogen activator inhibitor-1 within the porcine oviduct. *Biol Reprod* 2000; 62: 501-510.
92. Lopez-Ubeda R, Garcia-Vazquez FA, Romar R, *et al.* Oviductal transcriptome is modified after insemination during spontaneous ovulation in the sow. *PLoS One* 2015; 10: 0130128. doi: 10.1371/journal.pone.0130128
93. Schatz F, Lockwood CJ. Progestin regulation of plasminogen activator inhibitor type 1 in primary cultures of endometrial stromal and decidual cells. *J Clin Endocrinol Metab* 1993; 77: 621-625.
94. Carpene C, Dray C, Attane C, *et al.* Expanding role for the apelin/APJ system in physiopathology. *J Physiol Biochem* 2007; 63: 358-373.
95. Takakura N, Kidoya H. Maturation of blood vessels by haematopoietic stem cells and progenitor cells: involvement of apelin/APJ and angiopoietin/Tie2 interactions in vessel caliber size regulation. *Thromb Haemost* 2009; 101: 999-1005.
96. Kourtis A, Gkiomisi A, Mouzaki M, *et al.* Apelin levels in normal pregnancy. *Clin Endocrinol* 2011;75: 367-371.

Received: October 15, 2021
Accepted: December 31, 2021

Author's address: Prof. Anita Franczak, Department of Animal Anatomy and Physiology, Faculty of Biology and Biotechnology, University of Warmia and Mazury in Olsztyn, 1A Oczapowskiego Street, 10-719 Olsztyn, Poland.
E-mail: anitaf@uwm.edu.pl